Bandwidth enhancement of cylindrical triangular microstrip antenna using a stacked technique

Essam Salem Al-Sayed[*] and Nabeel Abbas Areebi
Department of Physics, College of Education, Al-Qadisiyah University, Al-Qadisiyah 58002, Iraq

E-mail: esammosa218@gmail.com

Abstract
This paper presents a new design of a conformal microstrip antenna operating in a dual-band for several applications including Wireless Local Area Networks (WLAN), Wi-Fi networks, and Wireless Body Area Networks (WBAN). The proposed design was achieved using the stacked patch technique on a conformal microstrip antenna. One of the patches is square-shaped and the other is triangular-shaped constructed on a cylindrical surface with a 50 mm radius using a substrate with a permittivity of 2.98. The proposed design can be called a stacked square-shaped triangular cylindrical microstrip antenna. The operating resonant frequencies have been set at 623 and 795 GHz. For the standard antenna, the bandwidths of dual-band are equal to 0.65% and 0.92%. By adding an air gap between the ground plane and substrate, bandwidths are enhanced to 6.15% and 3.07%, and then increasing the substrates' thickness leads to more improvement of the percentage of bandwidth to 40.2% and 24.12%. The Finite-Difference in Time Domain (FDTD) method is used to design and analyze the proposed antenna.

Keywords: microstrip antennas, dual-band, stacked path, bandwidth, air gap, finite-difference in time domain.

1. Introduction

An antenna is a conductor of electricity or a series of conductors used in a sending or receiving system to send or receive electromagnetic waves. A microstrip antenna is made up of two tiny superconductors between them dielectric substrates [1]. Therefore, there are two types of microstrip antennas; the first type is planar microstrip antennas and non-planar or conformal microstrip antennas. Conformal microstrip antennas with high directivity and low cost have a wide range of applications [2]. Although the major shapes examined so far are, cylindrical, spherical, and conical, conformal antennas can be practically any geometry. The simplest conformal antennas are those with a single curved surface [3]. Although the conducting patch can be any shape, rectangular and circular designs are the most frequent [4]. The triangle-shaped patch antenna is one of the recent shapes that has gotten a lot of attention. Figure 1 shows the geometric structure of a cylindrical triangular microstrip antenna (CTMA), where a represents the radius of the cylindrical ground, h represents the thickness of the cylindrical substrate with dielectric constant ε_r, and d_1

and d_2 represent the length of the sides of the triangle, while d_h represents the height of the triangle. The relationship between the dimensions of the patch triangle is [5]:

$$d_1 = \sqrt{((d_2/2)^2 + (2d_h)^2)}, \qquad (1)$$

The feed point will be at the point $(\emptyset_p, x_p)$ and the resonance frequency for mode TM_{mn} is given as [6]:

$$f_{mn} = 2c/(3d_1\sqrt{(\varepsilon_r)})\sqrt{(m^2 + mn + n^2)}, \qquad (2)$$

where m and n represent integers and c is the light speed in vacuum.

In many modern practical applications, dual-band of conformal microstrip antennas is required, such as the Internet of Things (IoT), wireless local area networks (WLAN), Wi-Fi networks, wireless body area networks (WBAN), military tracking, etc. [7]. In today's world of wireless communication networks, dual-band of antennas is extremely important. The latest wireless communication technology may deliver a high data rate and pervasive connectivity [8]. There are many ways to get an antenna operating in dual-band, for example, in 2001, Jan reported a dual-frequency circular microstrip
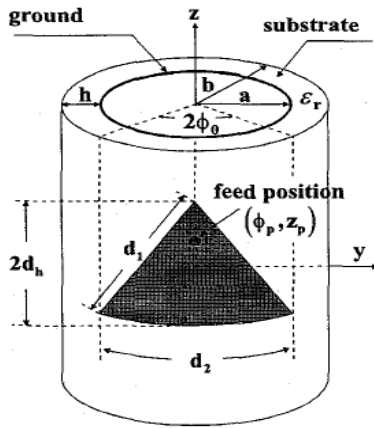
Figure 1. Geometry structure of CTMA.

Figure 2. Yee cells.

antenna design. It was loaded using an open ring slot and employed single-layer, single-feed [9].

In 2006, K.L. Wong et al. constructed an antenna with a T-shaped radiating structure, and two resonating modes are created by a radiating patch that is greater than the ground plane [10]. In 2010, H. Hsu et al. proposed an E-shaped patch antenna for wireless communication with two resonant frequencies of 2.4 and 3.5 GHz [11]. In 2012, R. Li, et al. offered an L-shaped and arc-shaped stub that serves as the radiating structure for a dual-band antenna [12]. In 2015, S. Liu et al. described the creation of stacked E-and U-shaped patches with peak gains of 7.1 and 7.4 dB for a dual-band operating at 2.6 and 3.5 GHz [13]. In 2017, Zhang and others presented a patch with double U-shaped elements, one of which is nested inside the larger U-shape [14].

In this paper, researchers will design a cylindrical triangular microstrip antenna of stacked square-shaped patch for double band operated at 6.2 and 8.6 GHz and enhance the bandwidth of dual-band. Most notably, the design and calculation were carried out in a finite deferent time-domain (FDTD) method using Matlab R2020a Program.

2. Theoretical part

The continuous development in technology led to many techniques for analyzing electromagnetic problems. These techniques can be divided into two types which are Analytical Techniques and Numerical Techniques [15]. Analytical techniques contributed to simplify engineering models and solving them in an integrated solution using different techniques, including Simple Cavity Model, Wire Grid Model, and Green Function Method [16]. The Finite Difference Time Domain Method FDTD, Finite Difference Frequency Domain Method FDFD, Method of Moments MoM, and Finite Element Method FEM are example for numerical techniques use to solve field equations which are directly subject to imposed boundary constraints by the geometric structure [17]. The FDTD method has a prominent place among the numerical techniques that were used in electromagnetic analysis over the last two decades. The FDTD method is extremely useful in simulating complicated structures because it
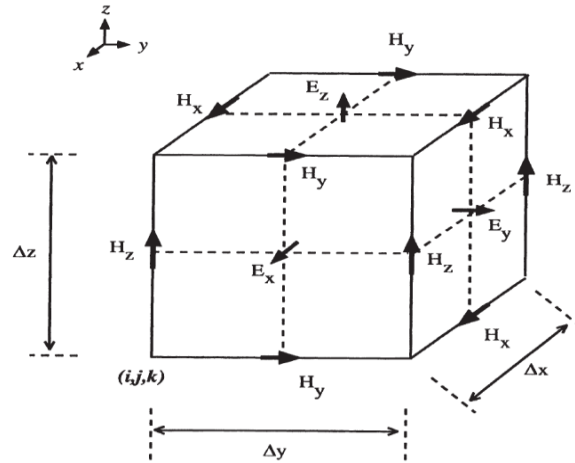
allows for direct integration of Maxwell equations depending on time as well as volume. Compared with the method of moment and the finite element method, the FDTD method is distinguished by the fact that it is a time domain technique. This means that a single simulation of the system leads to a solution that gives a wide response for a range of frequencies, using Fourier Transform Techniques. In addition to the above, some advantages of the FDTD method, It's good for simulations of broadband, It's good for structures of broadband, and It's highly scalable. One of disadvantages of FDTD method isn't good for structures of narrowband, i.e. cavity resonators and notch filters. K. Yee was the first to suggest the approach, and then others updated it in the early 1970s [7]. As shown in figure 2, Yee proposed that the FDTD space is made up of cells of identical size xyz called "Yee cells", and that the components of an electric and magnetic field are distributed around one cell in such a way that each component of an electric field is bounded by four components of a magnetic field, and each component of a magnetic field is bounded by four components of an electric field [18].

$$\nabla \times E = -\mu \frac{\partial H}{\partial t} + M, \qquad (3)$$

$$\nabla \times H = \frac{\partial D}{\partial t} + J, \qquad (4)$$

The curl operator generates coupled scalar equations and synonymous curl equations in the three-dimensional cylindrical coordinate system. Therefore, electric and magnetic fields in the x-direction obey the following equations [19]:

$$\frac{\partial E_x}{\partial t} = \frac{1}{\varepsilon} \left(\frac{\partial H_z}{\partial y} - \frac{\partial H_y}{\partial_z} - \sigma E_x \right), \qquad (5)$$

$$\frac{\partial H_x}{\partial t} = \frac{1}{\mu} \left(\frac{\partial E_y}{\partial z} - \frac{\partial E_z}{\partial y} - \rho H_x \right), \qquad (6)$$

By using partial derivatives of the second order with increments of time and space resulting from the Taylor series expansion [20], the two equations (5) and (6) can be written based on Finite Difference Notations [21]:
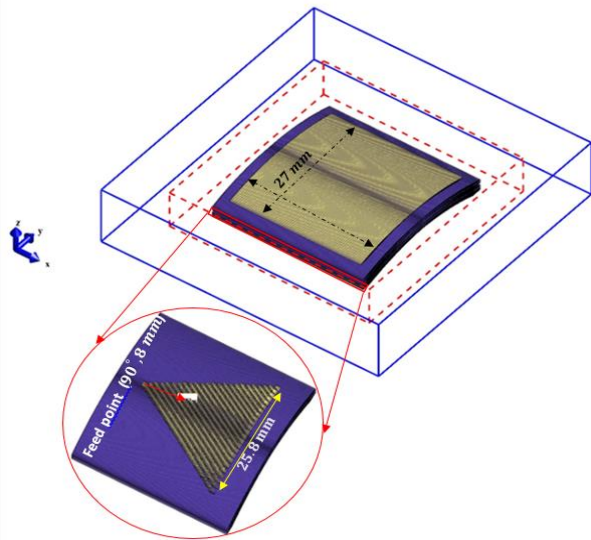
Figure 3. Structure of the proposed microstrip antenna.

$$E_x^{n+1}\left(i+\frac{1}{2},j,k\right) =$$

$$\left(\frac{\varepsilon(i,j,k)-\dfrac{\sigma(i,j,k)\Delta t}{2}}{\varepsilon(i,j,k)+\dfrac{\sigma(i,j,k)\Delta t}{2}}\right)E_x^n\left(i+\frac{1}{2},j,k\right)+$$

$$\frac{\dfrac{\Delta t}{\Delta y}}{\varepsilon(i,j,k)+\dfrac{\sigma(i,j,k)\Delta t}{2}}\left(\begin{array}{l}H_z^{n+\frac{1}{2}}\left(i+\frac{1}{2},j,k\right)-\\ H_z^{n+\frac{1}{2}}\left(i+\frac{1}{2},j-\frac{1}{2},k\right)\end{array}\right)-$$

$$\frac{\dfrac{\Delta t}{\Delta z}}{\varepsilon(i,j,k)+\dfrac{\sigma(i,j,k)\Delta t}{2}}\left(\begin{array}{l}H_y^{n+\frac{1}{2}}\left(i+\frac{1}{2},j,k-\frac{1}{2}\right)-\\ H_y^{n+\frac{1}{2}}\left(i+\frac{1}{2},j,k-\frac{1}{2}\right)\end{array}\right),$$

$$\hspace{10cm}(7)$$

$$H_x^{n+\frac{1}{2}}\left(i,j,k+\frac{1}{2}\right) =$$

$$\left(\frac{\mu(i,j,k)-\dfrac{\rho'(i,j,k)\Delta t}{2}}{\mu(i,j,k)+\dfrac{\rho'(i,j,k)\Delta t}{2}}\right)H_x^{n-\frac{1}{2}}\left(i,j+\frac{1}{2},k+\frac{1}{2}\right)-$$

$$\frac{\dfrac{\Delta t}{\Delta y}}{\mu(i,j,k)+\dfrac{\rho'(i,j,k)\Delta t}{2}}\left(E_z^n\left(i,j,k+\frac{1}{2}\right)-E_z^n\left(i,j-1,k+\frac{1}{2}\right)\right)+$$

$$\frac{\dfrac{\Delta t}{\Delta z}}{\mu(i,j,k)+\dfrac{\rho'(i,j,k)\Delta t}{2}}\left(E_y^n\left(i,j+\frac{1}{2},k\right)-E_y^n\left(i,j+\frac{1}{2},k-1\right)\right).$$

$$\hspace{10cm}(8)$$

Similar equations apply to the electric and magnetic fields in the y and z directions. The system is excited by an electrical impulse that is mathematically represented by a Gaussian function in the time domain called a Gaussian pulse [22]:

$$p(t) = e^{-(t-t_0)/\tau)^2}, \hspace{4cm} (9)$$

where τ is a damping factor that relates to the pulse width and has a value that varies based on the problem's frequency band and is the time of pulse delay. In the method of programming in infinite space, a perfectly matched layer is used. The values of the wave's compounds diminish and become very small as the wave propagates through space, compared to the values of the compounds at their greatest values. Fourier transformations can be used to calculate the values of impedance ($Z_{in} = R + iX$) after N calculations, where R and x represent resistance and recidivism, respectively. Input impedance in the frequency domain is [23].

$$Z_{in}=\left(\frac{\displaystyle\int_{-\infty}^{\infty}V(t)e^{-jwt}dt}{\displaystyle\int_{-\infty}^{\infty}I(t)e^{-jwt}dt}\right)=$$

$$\frac{\displaystyle\sum_{n=0}^{N}V(n\Delta t)e^{-jwn\Delta t}\Delta t}{\displaystyle\sum_{n=0}^{N-1}I\left(\left(n+\frac{1}{2}\right)\Delta t\right)e^{-jw\left(n+\frac{1}{2}\right)\Delta t}\Delta t} \hspace{1.5cm}(10)$$

where $V(t)$ is the voltage in the time domain calculated from Faraday's Law, and $I(t)$ is the electric current in the time domain calculated from Ampere's Law, and Return loss in the frequency domain calculated as [23]:

$$RL=\left(\frac{\displaystyle\int_{-\infty}^{\infty}V(t)e^{-jwt}dt}{\displaystyle\int_{-\infty}^{\infty}P(t)e^{-jwt}dt}\right)=$$

$$\frac{\displaystyle\sum_{n=0}^{N}V(n\Delta t)e^{-jwn\Delta t}\Delta t}{\displaystyle\sum_{n=0}^{N}P(n\Delta t)e^{-jwn\Delta t}\Delta t} \hspace{1.5cm}(11)$$

3. Geometry of antenna

Figure 3 shows the stacked square- and triangle-shaped patches of microstrip antenna calculated by the FDTD method. The antenna is designed to operate a dual-band at resonance frequencies 6.2 and 8.6 GHz.

The first patch is square with a side length equal to $L=27$ mm installed on a cylindrical dielectric substrate with a thickness of $h_1=0.562$ mm, type of RO 3003, and dielectric constant of $\varepsilon_{r1} = 2.98$. Whereas the second patch is an equilateral triangle with a side length of $d=25.8$ mm, installed on the same cylindrical dielectric substrate and a cylindrical radius $a=50$ mm, feed point F=8mm from the head of the triangle. The size of the ground plane is 30×30.8 mm. It is worth noting that the ground plane and patches are the same copper metal type and all the selected physical parameters were based on experimental work. The cell sizes were $\Delta x=\Delta y=0.871$ mm and $\Delta z=0.318$ mm, with a step time of $\Delta t=8.484\times10^{-12}$ S, determined by the relationship $c\Delta t \leq 1/\sqrt{(1/\Delta x)+(1/\Delta y)+(1/\Delta z)}$ [22]. The simulation had 20000 time steps
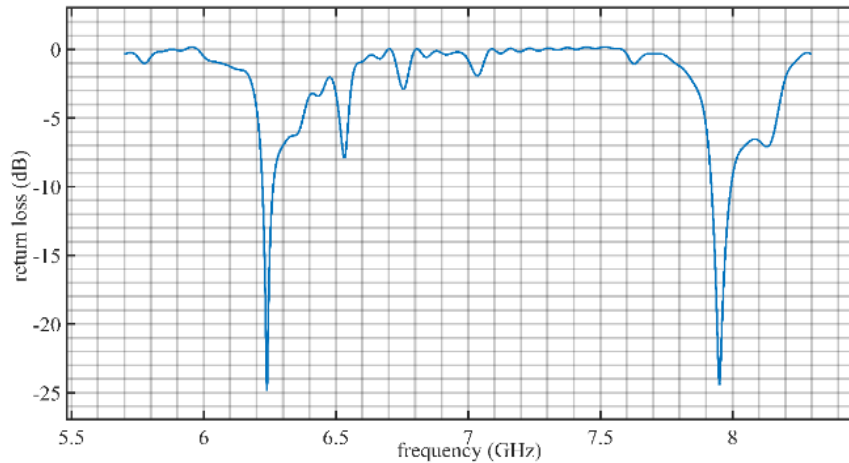
Figure 4. Return loss versus frequency by FDTD method ($h_1=h_2=0.562$ mm).
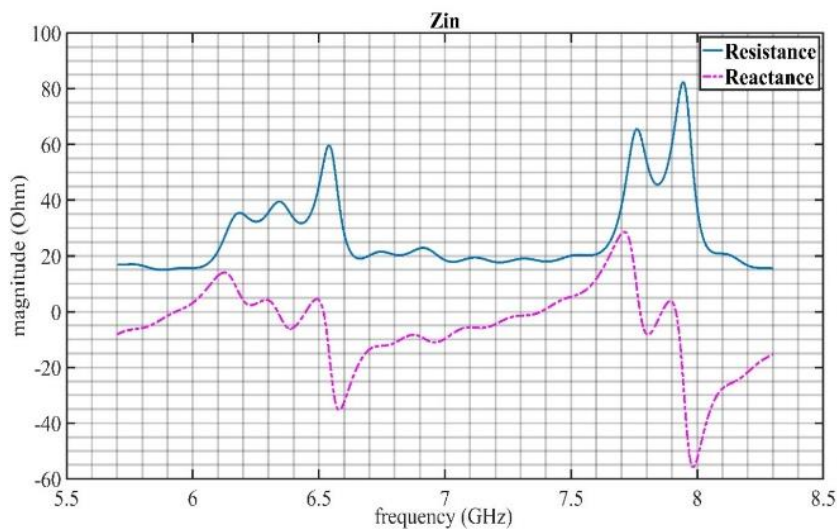
Figure 5. Input Impedance versus frequency by FDTD method ($h_1=h_2=0.562$ mm).

4. Results and discussions

The results below were obtained at the optimum feed point ($\emptyset_p=90^\circ$, $x_p=8$ mm) and the thickness of substrates are $h_1=h_2=0.562$ mm. From figure 4, it is clear that the antenna operates with a dual-band, the first band operates at $f_{r1}=6.23$ GHz and return loss equals to $RL_1=-24.87$ dB, the percentage of the first bandwidth is $BW_1=0.65\%$ and the second band operates at $f_{r2}=7.95$ GHz and return loss equal to $RL_2=-24.44$ dB, the percentage of the second bandwidth is $BW_2=0.92\%$.

The input impedance must be matched at 50 Ω for the antenna to perform efficiently since the first input impedance achieved results that were very close to 50 Ω ($Z_{in1}=50.2$ Ω) and the second input impedance achieved ($Z_{in2}=71$ Ω), as shown in figure 5.

4. 1 Enhancement of Dual-bandwidth

From figure 4, we notice that the bandwidth of the dual-band is relatively narrow. The researchers will try to enhance the dual-band to improve the performance of the proposed antenna by adding an air gap with a thickness of $h=0.5$ mm and a dielectric constant $\varepsilon_r = 1$ under the first dielectric substrate ($h_1=0.562$ mm , $\varepsilon_{r1} = 2.98$). In this
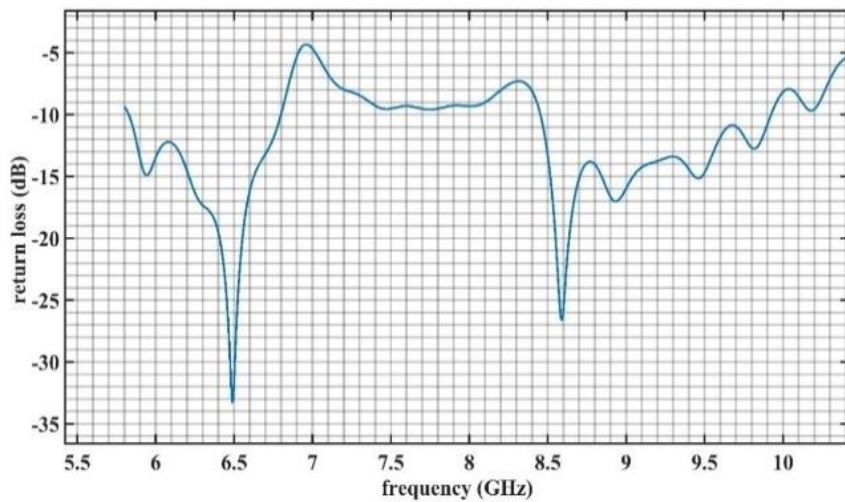
case, the thickness of the compound dielectric layer will increase to 1.062 mm, as for the dielectric constant, it is calculated from the relationship [24]:

$$\varepsilon_{reff} = \frac{\varepsilon_r \varepsilon_{r1}\left(h+h_1\right)}{\varepsilon_r h + \varepsilon_{r1} h_1}$$

(12)

Using the above equation, we find that the dielectric constant of the compound dielectric layer is less than that of the first layer, also the fringe fields have a great effect on the antenna performance. In microstrip antennas, the value of the electric fields was zero at the center of the patch, and the electromagnetic radiation could be produced from the created fringe fields between the patch and the ground plane of the antenna. It is important to mention that the amount of fringe fields depends on the antenna size as well as the thickness of the dielectric medium. As a result, the first resonance frequency occurs at $f_{r1}=6.5$ GHz with a bandwidth of $BW_1=6.15\%$ and return loss of $RL_1=-34$ dB, while at the second resonance frequency of $f_{r2}=7.88$ GHz, the bandwidth is $BW_2=3.07\%$, and return loss equals to $RL_2=-33.7$ dB, as seen in figure 6.
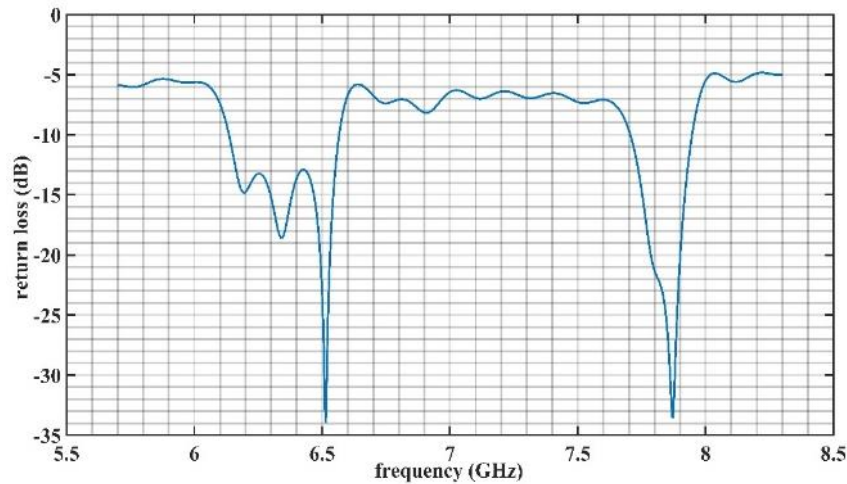
Figure 6. Return loss versus frequency by FDTD method with adding air gap $h=0.5$ mm, $h_1=h_2=0.562$ mm.

Figure 7. Return loss versus frequency by FDTD method with adding air gap $h=0.5$ mm, $h_1=h_2=0.762$ mm.

By increasing the thickness of the first and second dielectric substrates to $h_1=h_2=0.762$ mm, while the thickness of the air gap remains constant at $h=0.5$ mm, under the first dielectric substrate, the thickness of the compound dielectric layer increases to 1.262 mm, and the fringe fields increases as the thickness of the compound dielectric layer increases and from equation 12 we find that the dielectric constant of the compound dielectric layer is less than the dielectric constant of the first layer.

As a result of the decreased dielectric constant and increased thickness and fringe fields, the first bandwidth increases to $BW_1=15.34\%$, return loss is $RL_1=-33.23$ dB, while the second bandwidth becomes $BW_2=15.95\%$ and return loss equals $RL_2=-26.78$ dB, at the resonance frequency is $f_{r2}=8.6$ GHz, as seen in figure 7.

As shown in figure 8, by increasing the thickness of the first and the second dielectric substrates to $h_1=h_2=1$ mm, the thickness of the air gap remains constant at $h=0.5$ mm. In this case, the thickness of the compound dielectric layer will increase to 1.5 mm. As a result of increasing the thickness of the compound dielectric layer, the fringe fields increased, and from equation 12 we find that the dielectric constant of the

compound dielectric layer is less than the dielectric constant of the first layer. Because of this, the first bandwidth increases to $BW_1=31.45\%$, return loss equals $RL_1=-28$ dB and the resonance frequency becomes $f_{r2}=6.4$ GHz, while the second bandwidth becomes $BW_2=25.03\%$ with a returns loss of $RL_2=-24.13$ dB, and the resonance frequency increases to $f_{r2}=9.48$ GHz.

The best result is achieved at the substrates thickness of $h_1=h_2=1.262$ mm and air gap thickness of $h=0.5$ mm. In this case, the thickness of the compound dielectric layer increases to 1.762 mm, also the fringe fields increased as the thickness of the compound dielectric layer increased, from equation 12 we find that the dielectric constant of the compound dielectric layer is less than that of the first layer. As a result of the increased thickness, the fringe fields increased and the dielectric constant decreased, the result is shown in figure 9. The first bandwidth increase to $BW_1=40.2\%$, the return loss is $RL_1=-34.93$ dB, and the resonance frequency is equal $f_{r2}=6.47$ GHz. While second bandwidth becomes $BW_1=24.12\%$ and returns loss equal to $RL_2=-17.76$ dB, and the resonance frequency increases to $f_{r2}=9.68$ GHz. The results are summarized in table 1.
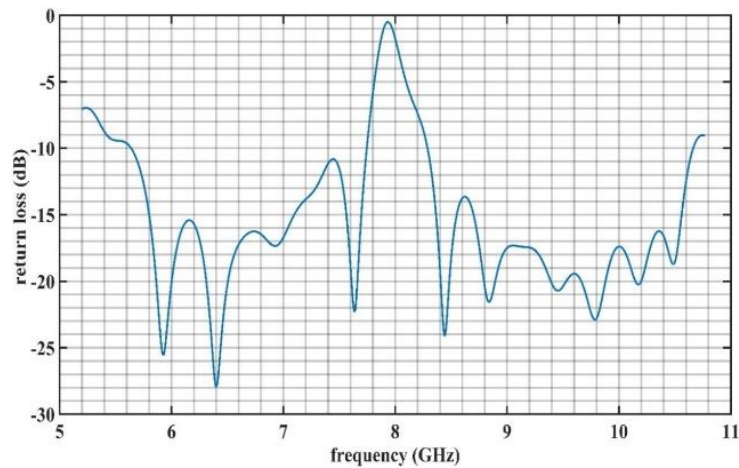
Figure 8. Return loss versus frequency by FDTD method with adding air gap $h=0.5$ mm, $h_1=h_2=1$ mm.
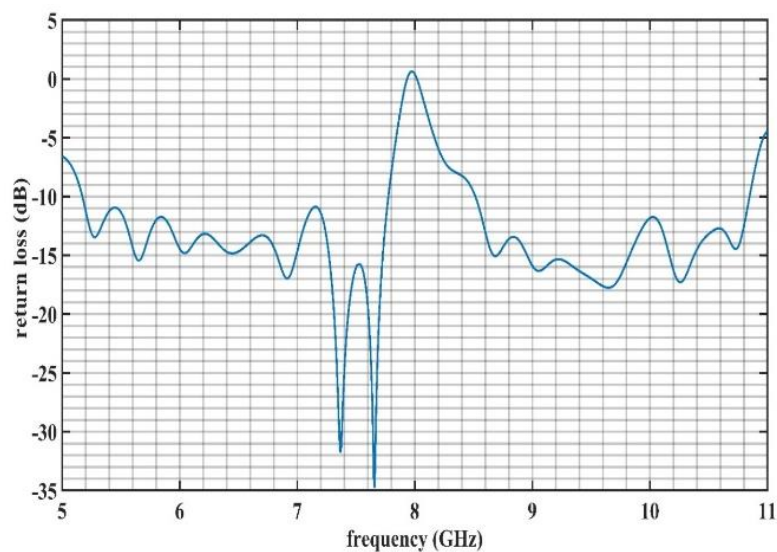
Figure 9. Return loss versus frequency by FDTD method with adding air gap $h=0.5$ mm, $h_1=h_2=1.262$ mm.

Table 1. Summary of the results.

d (mm)	L (mm)	a (mm)	F (mm)	Air gap (mm)	h_1, h_2 (mm)	$\varepsilon_{r1}, \varepsilon_{r2}$	BW$_1$ %	BW$_2$ %
27	25.8	50	8	-	0.562	2.98	0.65 %	0.92%
27	25.8	50	8	0.5	0.562	2.98	6.15 %	3.07%
27	25.8	50	8	0.5	0.762	2.98	15.34%	15.95%
27	25.8	50	8	0.5	1	2.98	31.45%	25.03%
27	25.8	50	8	0.5	1.262	2.98	40.2%	24.12%

5. Conclusions

The proposed antenna was designed using the FDTD method and simulated using the MATLAB program. The obtained results show that the stacked technique plays an important role to obtain a dual-band of microstrip antenna. Bandwidth increased by increasing the thickness of the dielectric layers and adding an air gap under the second dielectric substrate of the proposed antenna. We observed that using a stacked technique, air gap layer, and a thicker substrate is a good technique for enhancing the performance of microstrip antenna.

References

1. C A Balanis, "*Antenna theory: analysis and design*" John wiley & sons (2015).
2. R Mishra, *HCTL Open Int. J. Technol. Innov. Res.* **21**, 2 (2016) 1.
3. M V T Heckler and A Dreher, *IEEE Trans. Antennas Propag.* **59**, 3 (2011) 784.

4. N A. Areebi, Z A Ahmed, and M M Aubais, *Journal of Kufa−Physics* **12**, 1(2020) 1.

5. E Johari, *et al.*, *11th International Conference on Industrial and Information Systems, ICIIS 2016 - Conference Proceedings*, Roorkee, India (2016).

6. R Garg, *et al.*, "*Microstrip Antenna Design Handbook*", Artech house (2001).

7. E Balti and B K Johnson, *arXiv preprint arXiv:1901.05254* (2019).

8. E Li, X J Li, and B C Seet, *Electronics* **10**, 24 (2021) 3155.

9. J Y Jan, *Electro. Lett.* **37**, 16 (2001) 999.

10. K L Wong, Y C Lin, and T C Tseng, *IEEE Trans. Antennas Propag.* **54**, 1 (2006) 238.

11. H Hsu, F Kuo, and P Lu, *Microw. Opt. Technol. Lett.* **52**, 2(2010) 471.

12. R Li, *et al., Microw. Opt. Technol. Lett.* **54**, 6 (2012) 1476.

13. S Liu, W Wu, and D G Fang, *IEEE Antennas Wirel. Propag. Lett.* **15** (2015) 468.

14. X Y Zhang, *et al., IEEE Trans. Antennas Propag.* **65**, 1(2017) 103.

15. T H Hubing, "*Survey of Numerical Electromagnetic Modeling Techniques*" Department of Electrical Engineering, University of Missouri-Rolla, USA, (1991).

16. L W Abdullah, A H Sallomi, and M H Wali, *2021 IEEE 19th Student Conference on Research and Development (SCOReD)* (2021).

17. T Uno, *IEICE Trans. Commun.* **96**, 10 (2013) 2340.

18. W Bing, *IEEE Antennas and Propagation Society International Symposium,* IEEE (1997).

19. K Yee, *IEEE Trans. Antennas Propag.* **14**, 3 (1966) 302.

20. C Brunelli, H Berg, and D Guevorkian, *IEEE Workshop on Signal Processing Systems*, IEEE (2009).

21. A Elsherbeni, "*Time-Domain Method for Electromagnetics with MATLAB ® Simulations*". (2008).

22. D M Sheen, *Doctoral Dissertation*, Massachusetts Institute of Technology (1991).

23. I Transactions and O N Antennas, *IEEE Trans. Antennas Propag.* **36**, 1(1988) 1510.

24. M M A Al-Hillo, *Ph.D Thesis*, College of Scinece, University of Basrah, Basrah, Iraq (2012).